ISSN 0030-400X, Optics and Spectroscopy, 2016, Vol. 121, No. 5, pp. 722–728. © Pleiades Publishing, Ltd., 2016.
Original Russian Text © I.V. Stanishevsky, S.M. Arabei, V.A. Chernyavskii, K.N. Solovyev, 2016, published in Optika i Spektroskopiya, 2016, Vol. 121, No. 5, pp. 770–777.

CONDENSED-MATTER SPECTROSCOPY

Characterization of the T_1 State of Porphyrin Molecules on the Basis of Numerical Modeling of Decrease and Increase of Fluorescence Intensity Kinetics

I. V. Stanishevsky[a, *], S. M. Arabei[a], V. A. Chernyavskii[a], and K. N. Solovyev[b]

[a] *Belarusian State Agrarian Technical University, Minsk, 220023 Belarus*

[b] *Stepanov Institute of Physics of National Academy of Science of Belarus, Minsk, 220072 Belarus*

**e-mail: ivanstanisheuski@mail.ru*

Received May 5, 2016

Abstract—For a number of porphyrin molecules, it was shown that their excitation by light pulses of a rectangular step shape and a certain duration led to experimentally observed dynamical decrease and increase of fluorescence kinetics due to changes in the population of the lower (metastable) triplet T_1 state. On the basis of exact analytical expressions for a three-energy-level model, a simple analytical relationships between the rate constants of intramolecular processes and experimentally measured parameters of the fluorescence kinetics were obtained. The three-dimensional isotropic orientation of the molecules in the framework of the chosen model was taken into account by numerical methods and allowed to simulate adequately the experimentally observed fluorescence kinetics. The T_1 state lifetimes of the studied porphyrin molecules in polymer matrices were determined from experimental curves using numerical methods for solving inverse problems. The obtained values correlated with literature data. Features and advantages of this approach were discussed.

DOI: 10.1134/S0030400X16110199

INTRODUCTION

Along with well-known methods of determining the triplet T_1 state lifetime of organic molecules based on the analysis of the phosphorescence decay (pulsed and phase-modulation ones [1]), there is another method allowing one to obtain the similar and other information by analyzing the kinetics of fluorescence excited by rectangular photopulses [2–4]. The intensity of the $S_0 \leftarrow S_1$-fluorescence reaches its maximum value at the initial moment of irradiation with a rectangular photoexcitation (PhE) pulse and, then, decreases exponentially to a certain stationary value. Such behavior of the kinetics is due to the transition of molecules initially excited in the $S_0 \rightarrow S_n$ channel to a relatively long-lived (metastable) lower triplet T_1 state; therefore, the decrease in the fluorescence intensity is due to the increasing population of this state. The effect was found to be purely photophysical and reversible and named "fluorescence fading" (FF) (photophysical fading) [2–4]. FF is associated with establishing the equilibrium population in the system of energy levels upon quasi-stationary PhE and its observation is possible at a nonzero efficiency of the T_1 state population through the intersystem crossing $S_n \rightsquigarrow T_1$. In addition, the rise time of the front of the rectangular PhE pulse should be much shorter than the lifetime of the triplet state. The method of determining the T_1 state lifetime based on the analysis of FF has certain advantages over traditional methods because it allows:

—to obtain information about the T_1 state lifetime even in the case in which phosphorescence is very weak or completely absent (due to purely nonradiative deactivation of the state);

—to improve the accuracy and expressiveness of the measurements since photodetectors are much more sensitive in the spectral range of fluorescense of a sample rather than its phosphorescence;

—to obtain data on lifetimes of triplet states of photo-isomeric forms having spectrally separated fluorescence bands in the case when their phosphorescence bands are overlapped spectrally (which often takes place because the S_1–T_1 energy intervals are generally non-correlated).

Recently, using analytical and numerical computer modeling the population dynamics of the S_0-, S_1-, and T_1-levels of a typical metalloporphyrin under quasi-stationary PhE has been studied [5–7]. The calculations have shown that, after a sharp decrease in intensity of stationary PhE, which results in a proportional abrupt decrease of the fluorescence intensity, its value should then increase exponentially reaching a certain constant level. This new effect, which is similar in its nature to the FF effect, has been named 'fluorescence

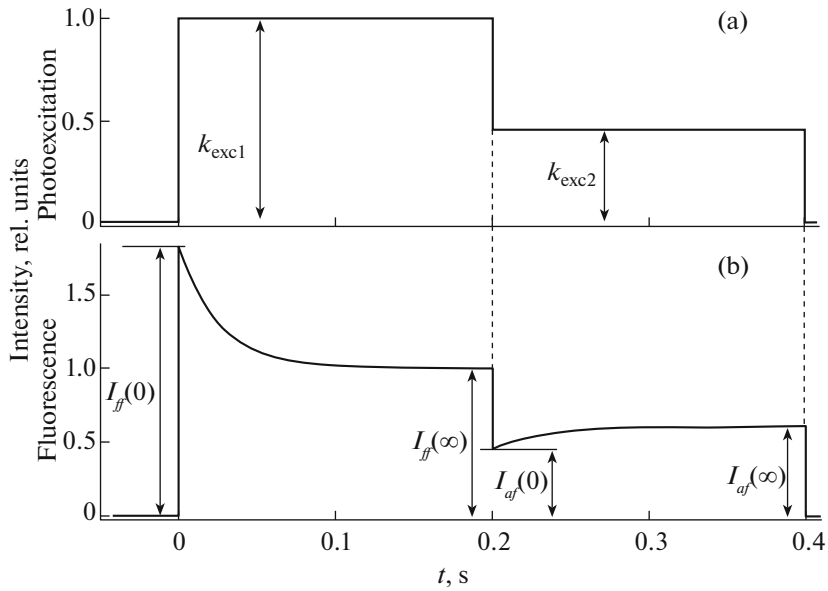

Fig. 1. (a) The shape of the two-step photoexcitation pulse; (b) schematic representation of FF and AF kinetics for a hypothetical metalloporphyrin molecule ($k_{exc1} = 18.5\ s^{-1}$, $k_{exc2} = 8.5\ s^{-1}$, $p = 22\ s^{-1}$, $f = 10^7\ s^{-1}$, and $k_{ST} = 5 \times 10^8\ s^{-1}$).

antifading' (AF). The AF effect has been confirmed experimentally by observation of the fluorescence kinetics of a zinc-tetrabenzoporphyrin complex in a polymer matrix at 300 [5, 6] and 77 K [7]. Note that FF and AF effects following each other have been experimentally observed with the help of using of modulated laser diode generated a sequence of two-step PhE pulses of descending intensity.

In the present work, a method based on the study of the FF and AF kinetics is applied for characterization of the T_1 state of a number of chlorophyll-like molecules at 77 K. The relation between the rate constants of intramolecular processes and experimentally measured parameters of fluorescence kinetics is presented in the theoretical section. Approximation to a real experimental data is based on numerical modeling of the population dynamics of electronic energy levels. In calculations, the isotropic spatial orientation of the molecules is considered in the same way as it has been done in [7–9]. The simulated and experimental fluorescence kinetics are treated using modern numerical inverse problem methods, which allows us to obtain most reliable information on the T_1 state of the studied molecules and intramolecular processes with its participation.

MODELING OF FF AND AF PROCESSES

The analytical solution of system of balance (ordinary differential) equations (1) describing the population kinetics of the electronic S_0-, S_1-, and T_1 states of an organic fluorophore under quasi-stationary PhE taking into account the normalization and closure conditions ($[S_0(t)] + [S_1(t)] + [T_1(t)] = 1$) allows to obtain the exact expression for the $[S_1(t)]$ population, and, thus, for fluorescence intensity $I(t)$ ($I(t) \sim [S_1(t)]$) [10],

$$\begin{cases} \dfrac{d[S_0]}{dt} + k_{exc}[S_0] - f[S_1] - p[T_1] = 0, \\ \dfrac{d[S_1]}{dt} - k_{exc}[S_0] + (f + k_{ST})[S_1] = 0, \\ \dfrac{d[T_1]}{dt} - k_{ST}[S_1] + p[T_1] = 0. \end{cases} \quad (1)$$

Here, k_{exc}, f, k_{ST}, and p are, respectively, the rate constant of PhE, the total rate constant of the $S_1 - S_0$ deactivation channel, the rate constant of the intersystem crossing $S_1 \rightsquigarrow T_1$, and the total rate constant of the T_1 state deactivation. Note that the splitting of the triplet T_1 level to its sublevels is not considered. Symbolic calculations were performed using the Maxima program [11].

Figure 1 schematically shows the calculated profile of two-step PhE (a) and fluorescence kinetics $I(t)$ of a hypothetical metalloporphyrin (b) obtained in the approximation of one-dimensional model (1). Note also that, for the intensity notions shown in Fig. 1b, relative intensity changes δ of the FF and AF processes can be defined as $\delta_{ff} = [I_{ff}(0) - I_{ff}(\infty)]/I_{ff}(\infty)$ and $\delta_{af} = [I_{af}(0) - I_{af}(\infty)]/I_{af}(\infty)$, respectively.

Under certain assumptions, the equation for $[S_1(t)]$, the form of which is rather cumbersome, can be simplified to a reasonably accurate expression for δ (δ_{ff} and δ_{af}), as well as for the characteristic times of the

FF and AF processes (τ_{ff} and τ_{af}), which are the same for both processes [6]:

$$\delta = \frac{k_{\text{exc}} Q_{ST}}{p}[S_0(0)] - [T_1(0)], \quad (2)$$

$$\tau = \frac{1}{p + k_{\text{exc}} Q_{ST}}. \quad (3)$$

The Q_{ST} parameter, under conditions of a low PhE intensity ($k_{\text{exc}}/f \ll 1$) and metastability of the T_1 level (for porphyrins, p/f and $p/k_{ST} \ll 1$ are typically 10^{-5}) is close in its value to the quantum yield of the intersystem crossing Φ_T: $\Phi_T = k_{ST}/(f + k_{ST})$. For example, if the metastability condition is satisfied and a typical ratio $k_{\text{exc}}/f \approx 10^{-5}$, then $|Q_{ST} - \Phi_T| \approx 10^{-5}$. The $[S_0(0)]$ and $[T_1(0)]$ are the populations of the electronic levels at the time moment of PhE intensity switching on or change.

If we consider the starting point of FF ($t = 0$), for which $[S_0(0)] = 1$ and $[T_1(0)] = 0$, and taking into account (2), then expression (3) for the characteristic time of FF can be written in the form

$$\tau_{ff} = \frac{1}{p(1 + \delta_{ff})}. \quad (4)$$

Using the relationship between τ_T and p, i.e., $\tau_T = p^{-1}$, the expression (4) gives

$$\tau_T = (1 + \delta_{ff})\tau_{ff}. \quad (5)$$

Since

$$1 + \delta_{ff} = \frac{I_{ff}(0)}{I_{ff}(\infty)}, \quad (6)$$

expression (5) with (6) can be written as

$$\tau_T = \frac{I_{ff}(0)}{I_{ff}(\infty)}\tau_{ff}. \quad (7)$$

Thus, to obtain τ_T, it is necessary to derive from the experimental (or simulated in the case of numerical simulation) curve of the FF kinetics the values of $I_{ff}(0)$, $I_{ff}(\infty)$, and τ_{ff}. Expression (7) is simpler and clearer than those given in [2–4]. Taking into account the normalization and closure conditions, as well as validity of the nonequalities $[S_0(t)]$, $[T_1(t)] \gg [S_1(t)]$ that follow from the values of the intramolecular rate constants given in Fig. 1, the relationship between the intensities and populations of the S_0 and T_1 levels may be represented as

$$\frac{I_{ff}(0)}{I_{ff}(\infty)} = \frac{[S_0(0)]}{[S_0(\infty)]} = \frac{1}{1 - [T_1(\infty)]}. \quad (8)$$

The lifetime τ_T of the T_1 state can also be obtained from the kinetics of AF if, at the time moment when PhE intensity is abruptly reduced, the populations of the S_0-, S_1-, and T_1 levels are known. Because of the mutual coupling and continuity of the processes, their values are equal to the corresponding final values of the populations of the previous process. Using (2), (3), and (8), it can be shown that

$$\tau_T = \frac{I_{ff}(0)}{I_{ff}(\infty)}\frac{I_{af}(0)}{I_{af}(\infty)}\tau_{af}. \quad (9)$$

It is obvious that the uncertainty of determining the values of τ_T from the AF curve is larger than from the FF curve.

Expressions (7) and (9) were verified by analytical and numerical methods (numerical calculations were carried out using the Scilab package [12]) for a wide range of rate constant values of intramolecular processes, as well as PhE ones. For the PhE intensities which result in $\delta_{ff} \leq 1$, the values of τ_T, calculated using both analytical and numerical methods, were close to the values calculated using expressions (7) and (9). The relative discrepancy of the results obtained by the aforementioned methods typically did not exceed 10^{-6}.

Numerical simulation also showed that formulas (2), (3), (7), and (9) are valid for cases in which a multilevel energy model can be reduced to the three-level one. An example is the model in which excitation of high-lying excited singlet states ($S_0 \to S_n$ transitions) is followed by the population of the S_1 state via the process of internal conversion with participation of vibrational sublevels ($S_n \rightsquigarrow S_1$ transitions).

To model the kinetics of the FF and AF processes, which were supposed to be observed in real experiments, in the three-level model the spatial orientation of homogeneously distributed noninteracting absorbing and emitting oscillators was taken into account. As expected, the use of the three-dimensional model and numerical methods described in [8, 9] revealed a dispersion of the characteristic times of the FF and AF processes. A similar dispersion had been noted earlier for kinetics of studied photoprocesses [8].

In the present work, the numerically simulated in the framework of the three-dimensional three-level model FF and AF kinetic curves, as well as curves obtained experimentally at 77 K, were processed with the use of programs CONTIN [13] and FTIKREG [14]. Using different algorithms for solving the integral Fredholm equation of the first kind (10), these programs calculated the spectral density function of characteristic times $F(\tau)$ of the FF and AF processes

$$I(t) = \int_0^\infty F(\tau)\exp\left(-\frac{t}{\tau}\right)d\tau, \quad (10)$$

where $I(t)$ are studied dependences $I_{ff}(t)$ and/or $I_{af}(t)$.

Figure 2a shows the results for the spectral density of characteristic time $F(\tau)$ of FF and AF simulated kinetics, which are relative to those presented in Fig. 1b. The positions of the maxima of $F(\tau)$ for the three-dimensional model (curves *3* and *4* in Fig. 2a) exceeds the values of τ for the one-dimensional model

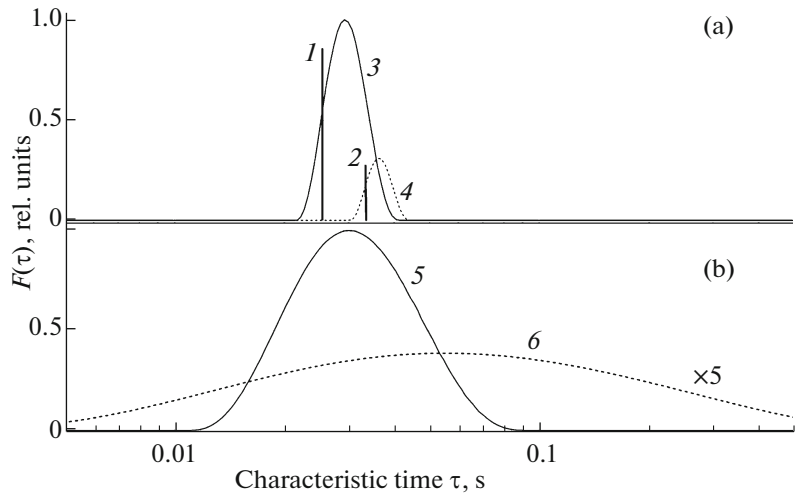

Fig. 2. Spectral density of characteristic times $F(\tau)$ of simulated (*1, 3, 5*) FF and (*2, 4, 6*) AF kinetics for a typical metalloporphyrin ($f = 1 \times 10^7$ s^{-1}, $k_{ST} = 5 \times 10^8$ s^{-1}, $p = 22$ s^{-1}, $k_{exc1} = 18.5$ s^{-1}, and $k_{exc2} = 8.5$ s^{-1}). (a) Calculations in the approximation of (*1, 2*) one- and (*3, 4*) three-dimensional models in the absence of the noise. (b) Calculations in the approximation of (*5, 6*) a three-dimensional model at a maximum amplitude of the noise equal to $\pm 0.033I(0)$.

(vertical lines *1* and *2* in Fig. 2a). This is because, in the one-dimensional model, k_{exc} is a constant, whereas in the three-dimensional model it takes values in the range from zero to k_{exc}. In fact, the light absorbing dipoles oriented at different polar angles Θ to the electric vector of the laser light are excited with probability $\sim\cos^2\Theta$. This results in a change of the effective value of k_{exc}. The difference in the maxima of the $F(\tau)$ bands (curves *3* and *4*) explains the expression (3). Simulation of kinetics with different $k_{exc}Q_{ST}/p$ values showed that the use of high intensities of PhE for which $\delta_{ff} \gg 1$ is inadvisable primarily because of the growing uncertainty of determination of the intensity ratios in expressions (7) and (9) and, respectively, the values of τ_T. In addition, when $\delta \gg 1$, the $F(\tau)$ bands broaden and show a structure that, generally speaking, also complicates determination of the values of τ_T.

For a correct comparison of simulated kinetic curves with experimental ones, which are usually noisy, we added a controlled fraction of Poisson-type noise to the simulated (smooth) curves. As expected, this led to an additional broadening of the $F(\tau)$ bands (curves *5* and *6* in Fig. 2b), as well as to a shift of the positions of their maxima: the maxima of bands *3* and *5* as well as of bands *4* and *6* do not coincide slightly. For curves *4* and *6*, the mismatch of the $F(\tau)$ band maxima is more pronounced than for curves *3* and *5* due to a lower 'signal-to-noise' ratio for the AF kinetic curves as compared with FF one. Note that the noise in the original $I(t)$ curve is the main uncertainty source of determination of the $F(\tau)$ band position.

In addition, if inverse problem calculations yield an asymmetry or structure of the $F(\tau)$ bands, it may be advisable to determine the values of τ, not from the position of the $F(\tau)$ maximum, but from the position of the gravity center of the band or a group of bands.

Note that the $I_{ff}(\infty)/I_{af}(0)$ ratio should be strictly equal to the intensity ratio of the steps in the PhE pulse (k_{exc1}/k_{exc2} in Fig. 1a). This allows to control the parameters of PhE pulses as well as photophysics of the observed processes. A possible reason for discrepancy in the values of the ratios could be, in particular, the presence of the stimulated emission. Preliminary calculations show that the simulated emission increases the $I_{ff}(\infty)/I_{af}(0)$ ratio, leaving the accuracy of determination of τ_T practically unaffected. The ratio also allows to control the photophysics of the FF and AF processes by comparing the corresponding distributions of $F(\tau)$.

The features of the FF and AF processes established in the course of the numerical simulation were further used in the analysis of experimental data and their interpretation.

OBJECTS AND METHODS OF RESEARCH

The objects studied were synthetic tetrapyrrole compounds: Zn tetrabenzoporphyrin (ZnTBP), Zn tetra-*tert*-butyl-tetrabenzoporphyrin (Zn $(tBu)_4$-TBP), and free base porphyrin (H_2P), dihydroporphyrin (chlorin, H_2C), *meso*-tetrapropylchlorin (H_2TPrC), *meso*-tetraphenylporphyrin (H_2TPP), *N*-methyl-*meso*-tetraphenylporphyrin (*N*-CH_3-TPP), *meso*-tetra(sulfonatophenyl)porphyrin (H_2TSPP), and tetra-*tert*-butyl-tetraazaporphyrin (H_2-$(tBu)_4$-TAP). Structural formulas of some studied compounds are given in the inserts of Fig. 3 and 4. The experimental samples were polymer films of polyvinyl butyral (PVB)

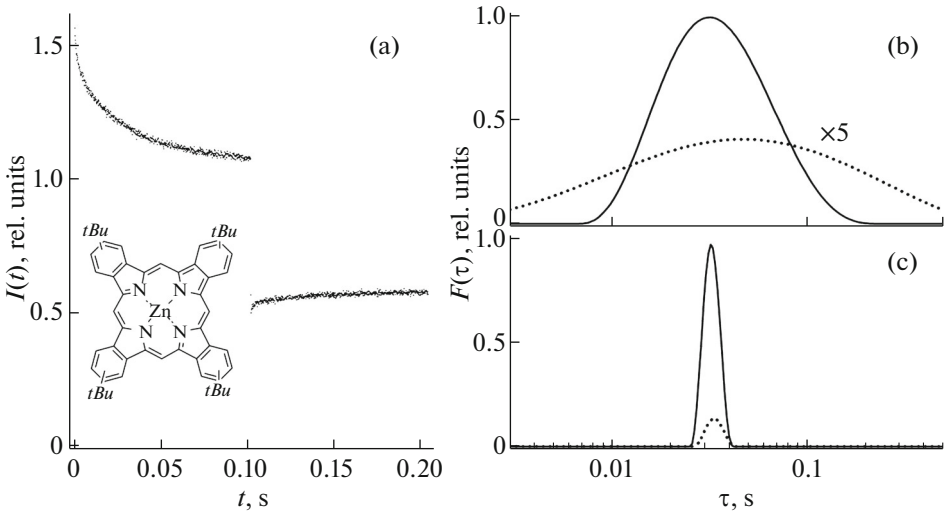

Fig. 3. (a) Experimental curves of FF and AF kinetics of Zn $(tBu)_4$–TBP in PVB at 77 K. Calculated spectral density of characteristic times $F(\tau)$ for (b) noisy and (c) smoothed with the Daubechies wavelet filter experimental curves of the FF (solid lines) and AF (dashed lines) kinetics.

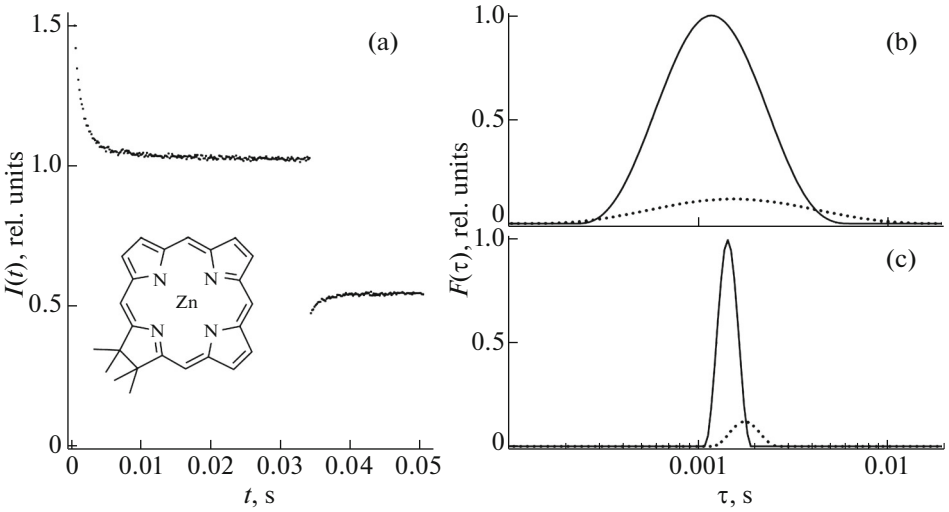

Fig. 4. (a) Experimental curves of FF and AF kinetics of H_2C in PVB at 77 K. Calculated spectral density of the characteristic times $F(\tau)$ for (b) noisy and (c) smoothed with the Daubechies wavelet filter experimental curves of the FF (solid lines) and AF (dashed lines) kinetics.

or polystyrene (PS), of the 100–200 μm thickness obtained by the irrigation method and colored with the aforementioned pigments (~10^{-5} mol/L). All spectral and kinetics measurements were performed at 77 K.

A laser diode (similar to SANYO DL4146-101S, $\lambda_{exc} \approx 405$ nm) with a radiation power of few mW, driven by a generator of current pulses of a two-step rectangular shape and with the front rise and fall time of ≈50 ns (the shape of the light pulse is schematically shown in Fig. 1a) was used as a photoexcitation source. The duration of the steps and the ratio of their amplitudes could be set independently. The sample fluorescence was detected in the spectral range of the 0–0 band of the studied objects using PMT (PM943-02, Hamamatsu, Japan). More detailed information on the detection method of the kinetic curves and data collection is given in [6]. Some additional changes were made in the experimental setup described in [6]; they included installation of a more efficient heatsink for the laser diode; application of the AD8065 operational amplifier to convert the PMT current to voltage

Lifetimes of the T_1 state (τ_T) of the studied porphyrins

Compound/matrices	λ_{det}, nm	τ_T, ms		τ_T, ms; (matrices) [reference]
		FF	AF	
Zn TBP/PVB	629	45 ± 7	46 ± 8	40 (EPA*) [15], 52 ± 10 (octane) [16]
Zn $(tBu)_4$-TBP/PVB	630	48 ± 7	50 ± 8	
H_2P/PVB	614	6.7 ± 1.0	6.8 ± 1.2	11.5 (PEP**) [15], 11 (octane + benzene) [17]
H_2C/PVB	635	2.0 ± 0.3	2.1 ± 0.3	5 (?) [18]
H_2TPC/PVB	652	1.1 ± 0.15	1.1 ± 0.15	
H_2TPP/PVB	645	3.7 ± 0.6	3.8 ± 0.6	5.6 (PEP) [15]
H_2TSPP/PVB	645	4.2 ± 0.6	4.3 ± 0.7	
N-CH_3-TPP/PS	676	0.65 ± 0.15	0.70 ± 0.20	
$H_2(tBu)_4$-TAP/PVB	620	0.85 ± 0.15	0.90 ± 0.20	1.4 (EPIP***) [19]

*EPA—ethyl ether–petroleum ether–ethanol (5 : 5 : 2).
**PEP—petroleum ether–propanol (1 : 1).
***EPIP—diethyl ether–petroleum ether–isopropanol (5 : 5 : 2).

and the PIC18F2458 microcontroller for the analog-to-digital conversion.

EXPERIMENTAL RESULTS AND DISCUSSION

Typical time dependences of the FF and AF intensities under excitation by laser pulses with the two-step rectangular shape are shown in Fig. 3a (Zn $(tBu)_4$–TBP in PVB, λ_{reg} = 630 nm) and Fig. 4a (H_2C in PVB, λ_{reg} = 635 nm). Note that in comparison with the results of [6], the lifetimes of fluorescence decay and recovery are longer because quenching of the T_1 state of porphyrins by molecular oxygen is vanishingly small at 77 K.

Figures 3b and 4b show the spectral density of characteristic times $F(\tau)$ of the FF and AF experimental curves depicted in Fig. 3a and 3b, respectively. The position and the mutual shift of the maxima of the $F(\tau)$ bands for Zn $(tBu)_4$-TBP and H_2C samples agree well with the results that follow from expressions (3) and numerical calculations performed using the intramolecular rate constants known for these compounds. The appearance and broadening of the $F(\tau)$ bands, in particular those shown in Fig. 3b, bear a significant similarity with the simulated curves presented in Fig. 2b. This indicates the adequacy of the numerical calculations performed with the use of the three-dimensional model.

Figures 3c and 4c show the dependences of $F(\tau)$ for experimental kinetic curves that were smoothed using a Daubechies wavelet filter. As seen, the noise removal leads to a significant narrowing of the $F(\tau)$ bands of FF and AF, as well as to small relative shifts of their maxima (in opposite directions in some cases). This result corresponds completely to the numerical calculations described above (Fig. 2). However, it should be noted that, in almost every case, to obtain optimal results requires selection or adjustment of the filter parameters, which complicates its routine use to some extent. In general, all experimental dependences $F(\tau)$ are in good agreement with those calculated for the simulated kinetics in the approximation of the three-dimensional model.

In the end, the values of τ_{ff} and τ_{af} were determined from maxima of the $F(\tau)$ bands of FF and AF. Intensities $I_{ff}(0)$, $I_{ff}(\infty)$, $I_{af}(0)$, and $I_{af}(\infty)$ were measured from the corresponding experimental kinetic curves of FF and AF. The lifetimes of the T_1 state, τ_T, were calculated according to relations (7) and (9). The values of τ_T obtained from the kinetic dependences of FF and AF are presented in the table where literature data are given for comparison.

As seen from the table, there is a difference in the τ_T values obtained from the FF and AF kinetics, which is mainly associated with more than a twofold smaller signal-to-noise ratio for the kinetic curves of AF. As it follows from numerical calculations, the maximum of the $F(\tau)$ spectrum shifts to larger time values as the noise of the kinetic curve increases (compare the pair of curves *3* and *5* with *4* and *6* in Fig. 2), which explains the differences in the τ_T values. The obtained τ_T values for the range of studied compounds are in a good qualitative agreement with literature data [15–19], while some deviations may be associated with the influence of the environment (solvent, polymer) and inaccuracy of the manual data processing in the early works.

It is important to note that the elaborated fluorescence method allows to carry out confident determi-

nation of τ_T of many free base porphyrins, the phosphorescence intensity of which is known to be very weak. In particular, τ_T for H_2TPP in alcohol-ether medium according to [15] is 5.6 ms. According to our data, the triplet T_1 state of this compound in PVB at 77 K has a shorter lifetime (see table). In addition, τ_T of H_2TPP is less than that of its sulfonated analog, and both values are confidently defined. It should be emphasized that the $F(\tau)$ dependences of the studied free bases exhibit no bands which could be assigned to the NH tautomerism processes.

CONCLUSIONS

In the course of this work, we identified and formulated several methodological advantages of the developed method based on pulsed two-step photoexcitation and observation of kinetics of the coupled FF and AF processes to determine the lifetimes of the lower metastable state and analyze the photoprocesses occurring in the system. A combined analysis of the coupled kinetic curves allows one to improve the reliability of determination of τ_T. A noticeable deviation of the parameters derived from the experimental curves and calculated ones may be an useful characteristic of the studied system. For example, it may indicate that the three-level model is not applicable to the real system. It should be noted that the specific form of the fluorescence signal (FF and AF curves) can unambiguously indicate on the presence in the system of fluorophores with a populated metastable state and, more importantly, even in the case in which their phosphorescence is absent. The use of two-stage PhE allows one to distinguish the fluorescence from other possible types of secondary emission owing to the unique profile of the kinetics ("signature of the process") exhibiting the decay and rise stages. The method of simulation of the FF and AF experimental curves seems to be promising to study the properties of the lower triplet states of organic fluorophores, as well as metastable states of any nature in other systems. Also, the numerical simulation approach is seen to be helpful for detection and identification of the presence of fluorophores in model and biological systems and can be a basis for development of a new luminescent method for quantitative and qualitative analysis of substances.

REFERENCES

1. J. Lakovich, *Principles of Fluorescent Spectroscopy* (Plenum, New York, 1986).
2. R. Avarmaa, Mol. Phys. **37**, 441 (1979).
3. L. Benthem, R. B. M. Koehorst, and T. J. Schaafsma, J. Mol. Struct. **79**, 455 (1982).
4. K. Mauring, I. Renge, P. Sarv, and R. Avarmaa, Spectrochim. Acta A **43**, 507 (1987).
5. I. V. Stanishevsky, K. N. Solovyev, S. M. Arabei, and V. A. Chernyavskii, in *Proceedings of the 4th Congress of Belarus Physicists* (Kovcheg, Minsk, 2013), p. 216.
6. I. V. Stanishevsky, K. N. Solovyev, S. M. Arabei, and V. A. Chernyavskii, J. Appl. Spectrosc. **80**, 357 (2013).
7. I. V. Stanishevsky, V. A. Chernyavskii, S. M. Arabei, and K. N. Solovyev, in *Proceedings of the 10th International Conference on Quantum Electronics* (RIVSh, Minsk, 2015), p. 242.
8. I. V. Stanishevsky and K. N. Solovyev, Opt. Spectrosc. **97**, 221 (2004).
9. I. V. Stanishevsky and V. A. Chernyavskii, J. Appl. Spectrosc. **82**, 726 (2015).
10. I. V. Stanishevsky and K. N. Solovyev, J. Appl. Spectrosc. **65**, 552 (1998).
11. Maxima. https://en.wikipedia.org/wiki/Maxima_(software).
12. Scilab. https://en.wikipedia.org/wiki/Scilab.
13. S. W. Provencher, Comput. Phys. Commun. **27**, 213 (1982).
14. C. Elster, J. Honerkamp, and J. Weese, Rheol. Acta **30**, 161 (1992).
15. A. T. Gradyushko and M. P. Tsvirko, Opt. Spektrosk. **31**, 548 (1971).
16. L. Bajema, M. Gouterman, and C. B. Rose, J. Mol. Spectrosc. **39**, 421 (1971).
17. M. P. Tsvirko, K. N. Solovyev, A. T. Gradyushko, and S. S. Dvornikov, Opt. Spectrosc. **38**, 400 (1975).
18. M. Gouterman, in *The Porphyrins,* Vol. 3: *Physical Chemistry, Part A,* Ed. by D. Dolphin (Elsevier, Academic, 1978), p. 1.
19. I. K. Shushkevich, V. N. Kopranenkov, S. S. Dvornikov, and K. N. Solovyev, J. Appl. Spectrosc. **46**, 368 (1987).